

GigaScience

Artifact-free whole-slide imaging with structured illumination microscopy and Bayesian image reconstruction --Manuscript Draft--

Manuscript Number:	GIGA-D-19-00306R1	
Full Title:	Artifact-free whole-slide imaging with structured illumination microscopy and Bayesian image reconstruction	
Article Type:	Data Note	
Funding Information:	National Institute of General Medical Sciences (1R15GM128166-01)	Dr Guy M Hagen
	Division of Biological Infrastructure (1727033)	Dr Guy M Hagen
Abstract:	<p>Background</p> <p>Structured illumination microscopy (SIM) is a method which can be used to image biological samples and can achieve both optical sectioning and super-resolution effects. Optimization of the imaging setup and data processing methods results in high quality images without artifacts due to mosaicking or due to the use of SIM methods. Reconstruction methods based on Bayesian estimation can be used to produce images with a resolution beyond that dictated by the optical system. Findings</p> <p>Five complete datasets are presented including large panoramic SIM images of human tissues in pathophysiological conditions. Cancers of the prostate, skin, ovary, and breast, as well as tuberculosis of the lung, were imaged using SIM. The samples are available commercially and are standard histological preparations stained with hematoxylin and eosin. Conclusion</p> <p>The use of fluorescence microscopy is increasing in histopathology. There is a need for methods which reduce artifacts when employing image stitching methods or optical sectioning methods such as SIM. Stitched SIM images produce results which may be useful for intraoperative histology. Releasing high quality, full slide images and related data will aid researchers in furthering the field of fluorescent histopathology.</p>	
Corresponding Author:	Guy M Hagen, PHD UNITED STATES	
Corresponding Author Secondary Information:		
Corresponding Author's Institution:		
Corresponding Author's Secondary Institution:		
First Author:	Karl A Johnson	
First Author Secondary Information:		
Order of Authors:	Karl A Johnson	
	Guy M Hagen, PHD	
Order of Authors Secondary Information:		
Response to Reviewers:	<p>Dear Editor:</p> <p>We would like to re-submit our manuscript entitled "Artifact-free whole-slide imaging with structured illumination microscopy and Bayesian image reconstruction" for consideration in GigaScience as a data note. We would like to thank the reviewers for their comments about the paper. Reviewer 1 was very enthusiastic about the paper and we appreciate these positive comments about our work. Reviewer 2 was also</p>	

positive, but had a few comments about the paper which were concerned with the organization of the paper and the data.

1. The first comment was that we should upload all of the un-stitched images, and to provide them as individual image files rather than as a single large file. This has been accomplished and now all of the raw and processed data is available at GigaDB. We packed all of the tiles for a given sample into ZIP files so that users will be able to download all of the tiles as a single large file. Otherwise users would have to click and download each file separately. GigaDB will probably re-package these files into a different format such as TAR.

2. The reviewer noted that we did not include certain information about the actual dataset in the main paper. For example, the directory structure, file sizes and types, etc. This information is not normally included in GigaScience articles which I have read. The GigaScience Instructions to Authors do not require this information. This information will be present on the GigaDB page for this dataset. There will be a table, generated by GigaDB, which will contain the desired information.

3. The reviewer noted that an open access dedication should be included with the dataset. This has been done.

4. The reviewer noted that, because the tissue preparations are of human origin, that information about ethics and consent should not be overlooked. Thank you for reminding us of this important point. However, because the samples were obtained commercially, it is the responsibility of the supplying company to ensure that ethical and legal guidelines are followed. I have double checked this with the Institutional Review Board (IRB) here at the University of Colorado, Colorado Springs. Because the samples are acquired commercially, and because they are completely de-identified (meaning that there is no way to connect these particular samples to the original donor), this is not considered human subject research, and approval is not required to work with these samples.

5, 6. In points 5 and 6, the reviewer is asking us to rearrange the paper by putting the items in the supplementary information into the main paper, and then to eliminate figures 7-10. Respectfully, we do not plan to do this for several reasons. I feel that reorganizing the manuscript as suggested would not improve the paper.

The whole point of the paper is to show the results of our research, in this case the results are the final, high resolution stitched images of the samples we examined. Eliminating these results from the paper would not be a good idea. For example, people working on breast cancer will be interested in the imaged breast cancer sample, people working on prostate cancer will be interested in the imaged prostate cancer sample, and so on. Further, the data re-use section was included in the supplementary material in our previous two papers in GigaScience. I believe this is the appropriate place for this information. Most GigaScience articles I have read do not include an actual, concrete example of data re-use like we do, and so this is a strength of our paper. Not everything can go into the main paper, and it is common practice today to publish supplementary information with additional experimental details, which can sometimes be quite lengthy.

Section 3 of the supplementary information is there for a specific reason. Almost all current research in structured illumination microscopy is performed on single cells using high magnification objectives. In the current paper we are imaging tissues over large areas, which is a quite different application. It is important for readers to realize that the methods presented here are widely applicable, including in the more typical application of SIM. Section 3 of the supplement is aimed at other people involved in the SIM field.

7. The structured illumination data processing steps are the same as were used in our previous publications. We noted this in the section 'SIM data processing' by stating that the SIM reconstructions were performed in the same way as previously described. What is new here is the image deconvolution and stitching methods applied to microscopy images of this type.

The steps described in the flow chart in Fig 3 are already described in the text. For example in the section 'SIM data processing' we state "SIM reconstructions were

	<p>performed using SIMToolbox...” and “We generated optically sectioned, enhanced resolution images using... MAP-SIM.” In the section ‘Vignetting correction’ we state “Following SIM reconstruction, ...We performed vignette removal by dividing each tile of the mosaic by an image representing the vignetting profile common to all tiles.” These are exactly the steps shown in the flowchart.</p> <p>8. The reviewer noted that the quality of figures 1, 3, and 5 is very low. This is perfectly true, in the PDF file they look absolutely terrible and it is very disappointing. However the problem is with the PDF conversion process used by GigaScience. This is not something that authors can change. Please click on the links embedded in the PDF (in the upper right corner of the pages containing the figures) to download the original high resolution files for the figures. You will see that they are of high quality.</p> <p>We hope that our paper will now be acceptable for publication in GigaScience.</p> <p>Sincerely,</p> <p>Guy M. Hagen</p>
Additional Information:	
Question	Response
Are you submitting this manuscript to a special series or article collection?	No
<p>Experimental design and statistics</p> <p>Full details of the experimental design and statistical methods used should be given in the Methods section, as detailed in our Minimum Standards Reporting Checklist. Information essential to interpreting the data presented should be made available in the figure legends.</p> <p>Have you included all the information requested in your manuscript?</p>	Yes
<p>Resources</p> <p>A description of all resources used, including antibodies, cell lines, animals and software tools, with enough information to allow them to be uniquely identified, should be included in the Methods section. Authors are strongly encouraged to cite Research Resource Identifiers (RRIDs) for antibodies, model organisms and tools, where possible.</p> <p>Have you included the information requested as detailed in our Minimum</p>	Yes

Standards Reporting Checklist?	
<p>Availability of data and materials</p> <p>All datasets and code on which the conclusions of the paper rely must be either included in your submission or deposited in publicly available repositories (where available and ethically appropriate), referencing such data using a unique identifier in the references and in the “Availability of Data and Materials” section of your manuscript.</p> <p>Have you have met the above requirement as detailed in our Minimum Standards Reporting Checklist?</p>	Yes

1 **Artifact-free whole-slide imaging with structured illumination microscopy**
2 **and Bayesian image reconstruction**

3 **Karl Johnson¹, Guy M. Hagen^{1*}**

4 ¹*UCCS center for the Biofrontiers Institute, University of Colorado at Colorado Springs*

5 *1420 Austin Bluffs Parkway, Colorado Springs, Colorado, 80918, USA*

6 [*ghagen@uccs.edu](mailto:ghagen@uccs.edu)

7 **Abstract**

8 **Background** Structured illumination microscopy (SIM) is a method which can be used to image biological
9 samples and can achieve both optical sectioning and super-resolution effects. Optimization of the imaging
10 setup and data processing methods results in high quality images without artifacts due to mosaicking or due
11 to the use of SIM methods. Reconstruction methods based on Bayesian estimation can be used to produce
12 images with a resolution beyond that dictated by the optical system.

13 **Findings** Five complete datasets are presented including large panoramic SIM images of human tissues in
14 pathophysiological conditions. Cancers of the prostate, skin, ovary, and breast, as well as tuberculosis of the
15 lung, were imaged using SIM. The samples are available commercially and are standard histological
16 preparations stained with hematoxylin and eosin.

17 **Conclusion** The use of fluorescence microscopy is increasing in histopathology. There is a need for methods
18 which reduce artifacts when employing image stitching methods or optical sectioning methods such as SIM.
19 Stitched SIM images produce results which may be useful for intraoperative histology. Releasing high quality,
20 full slide images and related data will aid researchers in furthering the field of fluorescent histopathology.

21 **Keywords** Structured illumination microscopy, SIM, image stitching, Bayesian methods, MAP-SIM,
22 SIMToolbox, histopathology, cancer.

23 **Data description**

24 **Context**

25 Structured illumination microscopy (SIM) is a method in optical fluorescence microscopy which can
26 achieve both optical sectioning (OS-SIM) [1] and resolution beyond the diffraction limit (SR-SIM) [2,3]. SIM has
27 been used for super-resolution imaging of both fixed and live cells [4–7] and has matured enough as a method that it
28 is now available commercially. In SIM, a set of images is acquired using an illumination pattern which shifts
29 between each image. As SIM has developed, diverse strategies have been proposed for creation of the SIM
30 pattern [1,8–13]. Several different approaches for processing the data have also been introduced [3,7,8,14–16].

31 Recently, microscope systems capable of imaging with high resolution and a large field of view (FOV)
32 have been developed [17–21], some using custom-made microscope objectives. However, stitching together images
33 acquired with a higher magnification objective to create a large mosaic remains a valid and popular approach. Some
34 published results involving stitched images suffer from pronounced artifacts in which the edges of the individual
35 sub-images are visible, usually as dark bands which outline each sub-image [22–24]. On the other hand, several
36 studies have proposed methods for stitching of microscope images with reduced artifacts [25–32].

37 The combination of SIM with image stitching methods allows collection of large FOV images with both
38 optical sectioning and super-resolution properties. Here, we demonstrate methods and provide complete datasets for
39 five different samples. The samples are hematoxylin and eosin (H&E) stained histological specimens which provide
40 examples of human diseases (ovarian cancer, breast cancer, prostate cancer, skin cancer, and tuberculosis), and
41 which are also available commercially for those who wish to reproduce our work. We used freely available optical
42 designs [6,10,33] and open source software [33] for SIM imaging, along with freely available software for image
43 stitching (Microsoft Image Composite Editor (ICE) [34], or a well validated plugin [26] for ImageJ [35]).
44 Combining this with deconvolution methods, we produced stitched images which are free of noticeable artifacts from
45 stitching or from SIM reconstruction.

46 Fluorescence microscopy is becoming more important in histopathology. Traditional bright field
47 microscopy diagnostic methods require a time-consuming process, involving chemical fixation and physical
48 sectioning. The use of optical sectioning fluorescence microscopy allows high-quality images to be captured without
49 the need for physical sectioning. Consequently, it has been shown that imaging can be performed on large human
50 tissue samples within 1 hour after excision [36]. Additionally, other studies have shown the results of fluorescence

51 imaging to be usable and accurate in diagnosis of various medical conditions [37–42]. Previously, it was noted that
 52 obvious stitching artifacts significantly decrease the usability of large fluorescence images in medical diagnosis. In
 53 one case, such artifacts resulted in the rejection of over half of the images acquired [38]. The setup we describe here
 54 allows for fast, artifact-free, high-resolution imaging of fluorescent samples, and is compatible with samples stained
 55 with most fluorescent dyes.

56 **Methods**

57 *Samples*

58 All samples used in this study are available from Carolina Biological, Omano, or Ward’s Science. The
 59 samples are approximately 7 μm thick and are stained with hematoxylin and eosin. The commercial source, product
 60 number, and other SIM imaging parameters for each sample are detailed in Table 1. Table 2 details imaging
 61 parameters for acquisitions of each sample with a color camera.

62 Table 1: Imaging parameters for the SIM datasets

Sample	Source company and product no.	SIM pattern no. of phases	Exposure time, ms	No. of tiles	Objective mag/NA	Acquisition time, s	Stitching software
Carcinoma of Prostate	Carolina, 318492	5	50	23 \times 11	20 \times /0.45	315	Microsoft ICE
Basal Cell Carcinoma	Ward’s Science, 470183-256	6	75	29 \times 18	30 \times /1.05	821	FIJI
Adenocarcinoma of Ovary	Carolina, 318628	5	100	25 \times 14	10 \times /0.4	595	Microsoft ICE
Adenocarcinoma of Breast	Carolina, 318766	8	200	12 \times 8	10 \times /0.4	278	FIJI
Lung Tuberculosis	Omano, OMSK-HP50	5	100	20 \times 16	30 \times /1.05	541	FIJI

63 Table 2: Parameters for the color images

Sample	No. of tiles	Objective mag/NA
Carcinoma of Prostate	6 \times 5	4 \times /0.16
Basal Cell Carcinoma	5 \times 5	4 \times /0.16

Adenocarcinoma of Ovary	11 × 11	4×/0.16
Adenocarcinoma of Breast	6 × 6	4×/0.16
Lung Tuberculosis	8 × 10	10×/0.4

64 *Microscope setup and data acquisition*

65 We used a home-built SIM setup based on the same design as described previously [6,10,15] (Fig. 1). The
66 SIM system is based on an IX83 microscope (Olympus) equipped with a Zyla 4.2+ sCMOS camera (Andor) under
67 the control of IQ3 software (Andor). We used the following Olympus objectives: UPLSAPO 4×/0.16 NA,
68 UPLSAPO 10×/0.4 NA, LUCPLFLN 20×/0.45 NA, and UPLSAPO 30×/1.05 NA silicone oil immersion. For color
69 images we used an aca1920-40uc color camera (Basler) under control of Pylon software (Basler). We used a MS-
70 2000 motorized microscope stage (Applied Scientific Instrumentation) to acquire tiled SIM images. In all datasets,
71 the stage scanning was configured such that all image edges overlapped by 20%.

72 Briefly, the SIM system uses a ferroelectric liquid crystal on silicon (LCOS) microdisplay (type SXGA-
73 3DM, Forth Dimension Displays). This device has been used previously in SIM and related methods in fluorescence
74 microscopy [5,10,15,33,43–47] and allows one to produce patterns of illumination on the sample which can be
75 reconfigured at will by changing the image displayed on the device. The light source (Lumencor Spectra-X) is
76 toggled off between SIM patterns and during camera readout. Close synchronization between the camera
77 acquisitions, light source, and microdisplay ensures rapid image acquisition, helps reduce artifacts, and reduces light
78 exposure to the sample. The supplementary material contains more information about system integration.

79 **INSERT FIGURE 1**

80 *SIM data processing*

81 SIM reconstructions were performed in the same way as previously described using SIMToolbox, an open-
82 source and freely available program that our group developed for processing SIM data [33]. We generated optically
83 sectioned, enhanced resolution images using a Bayesian estimation method, maximum *a posteriori* probability SIM
84 (MAP-SIM) [15]. MAP-SIM works using maximum *a posteriori* probability methods, which are well known in
85 microscopy applications [48,49], to enhance high spatial frequency image information. We then combine this
86 information, in the frequency domain, with low spatial frequency image information obtained by OS-SIM methods,

87 then produce the final image by an inverse Fourier transform [15]. We typically measure the final resolution
88 obtained by analyzing the frequency spectrum of the resulting image, as is discussed below.

89 The illumination patterns used here are generated such that the sum of all positions in each pattern set
90 results in homogenous illumination. As such, a widefield (WF) image can be reconstructed from SIM data simply by
91 performing an average intensity projection of the patterned images. This can be described by

$$92 \quad I_{WF} = \frac{1}{N} \sum_{n=1}^N I_n,$$

93 where N is the number of pattern phases, I_n is the image acquired on the n^{th} illumination position, and I_{WF} is the WF
94 reconstruction. This is the method we used to generate WF images throughout this study.

95 *Vignetting correction*

96 Following SIM reconstruction, vignetting artifacts remain in each tile. If not removed prior to stitching, this
97 vignetting introduces a distracting grid pattern in the final stitched image. We performed vignette removal by
98 dividing each tile of the mosaic by an image representing the vignetting profile common to all tiles. Other studies
99 have used an image of a uniformly fluorescent calibration slide as a reference for vignette removal [36], where
100 information concerning non-uniform illumination is captured. However, we found that SIM processing introduces
101 vignetting artifacts beyond those due to non-uniform illumination. Additionally, these artifacts vary depending on
102 properties of the sample being imaged. As such, performing pre-acquisition calibration on a uniformly fluorescent
103 slide is not sufficient to remove vignetting artifacts from SIM reconstructions. Instead, an estimate of the vignetting
104 profile is found through analysis of the mosaic tiles after SIM reconstruction.

105 A blurred average intensity projection of the tiles is a good approximation of the vignetting profile, as an
106 average intensity projection merges the tiles into a single image with reduced foreground information while
107 preserving vignetting. Subsequent blurring with an appropriate radius and edge-handling method also eliminates the
108 high spatial frequency foreground without impacting the low spatial frequency illumination profile. To eliminate
109 errors during the blurring step due to the blurring area extending outside the original image, we used an edge
110 handling method in which the blurring area is reduced near the edges of the image such that no values outside the
111 image border are sampled. Unlike edge handling methods in which the image is padded with a uniform value (or

112 mirrored and tiled) to accommodate a blurring area which extends beyond the original image limits, this method is
113 free from major artifacts, such as erroneous brightness of the image edges (see supplementary figure S1). This
114 approximation of the illumination profile works especially well for histological samples, as such samples are non-
115 sparse and require many tiles, factors which improve the accuracy this approach. We performed all steps of this
116 devignetting process using built-in functions and the ‘Fast Filters’ plugin in ImageJ [50]. The effect of devignetting
117 is illustrated in Fig. 2.

118 **INSERT FIGURE 2**

119 *Image Stitching*

120 With visible vignetting removed, we then stitched together a composite image from the tiles. The pre-
121 processing allows for stitching to be done in various stitching applications; Microsoft ICE and Preibisch’s plugin for
122 FIJI [26] were used to stitch the data presented here.

123 The data processing procedure is summarized in Fig. 3. The total time for processing each dataset was
124 about 30 min.

125 **INSERT FIGURE 3**

126 *Color image data processing methods*

127 We created color overview images by stitching devignetted brightfield acquisitions. Devignetting was
128 performed simply by adding the inverse of an empty brightfield acquisition to each color tile using ImageJ. For this
129 method to produce optimal results, the empty brightfield image must be acquired in conditions identical to those of
130 the raw tile data, such that the illumination profile in the empty image matches that of the unprocessed tiles. This
131 simple operation removes nearly all visible vignetting and color balance artifacts within each tile. The results after
132 devignetting were then stitched using Preibisch’s plugin for FIJI [26].

133 *Resolution measurement*

134 We evaluated our results by measuring image resolution using SR Measure Toolbox. SR Measure
135 Toolbox [51] measures the resolution limit of input images through analysis of the normalized, radially averaged
136 power spectral density (PSD_{ca}) of the images, as previously described [6]. Briefly, the resolution limit in real space

137 is determined by evaluating the cutoff frequency in Fourier space. The cutoff frequency is estimated by calculating
138 the spatial frequency at which the PSD_{ca} (after noise correction) drops to zero.

139 Focusing on the basal cell carcinoma sample, we selected 125 (out of 522 total) image tiles, calculated the
140 PSD and resolution for each tile, and averaged the results. We found that, in the case of this sample, the image
141 resolution was 593 ± 20 nm for WF and 468 ± 2.5 nm for MAP-SIM (average \pm standard deviation). This data was
142 acquired with a UPLSAPO 30 \times /1.05 NA silicone oil immersion objective. Figure 4 shows an example measurement
143 for one image tile. Figure 5 shows a plot of PSD_{ca} for this image tile.

144 **INSERT FIGURE 4**

145 **INSERT FIGURE 5**

146 **Results**

147 Figure 6 shows images of a prepared slide containing a human prostate carcinoma sample stained with
148 H&E. Fig. 6a shows a stitched color overview, and Fig. 6d shows a zoom-in of the region indicated in Fig. 6a,
149 acquired separately using a UPLSAPO 20 \times /0.75NA objective. Fig. 6b shows a stitched widefield fluorescence
150 image, and Fig. 6c shows a stitched SIM image. Figs. 6e and 6f each show zoom-ins of the stitches shown in Figs.
151 6b and 6c, respectively. Using the acquisition and processing methods described, whole-slide images are produced
152 without any visible stitching artifacts. Additionally, the MAP-SIM reconstruction method produces resolution
153 superior to that of the widefield data.

154 Figures 7-10 show similar comparisons for basal cell carcinoma, ovary adenocarcinoma, breast
155 adenocarcinoma, and tuberculosis of the lung, respectively.

156 The data shown in figures 6-10 is freely available through Giga DB [reference to be added]. This dataset
157 includes all color overviews as well as WF and MAP-SIM stitches at full resolution. In addition, all image tiles
158 (prior to deconvolution) used to create the WF and MAP-SIM stitches of the basal cell carcinoma sample are
159 provided.

160 **INSERT FIGURE 6**

161 **INSERT FIGURE 7**

162 **INSERT FIGURE 8**

163 **INSERT FIGURE 9**

164 **INSERT FIGURE 10**

165 **Discussion**

166 Many past studies into stitching of SIM mosaics have suffered from noticeable image artifacts, arising from
167 flaws in the optical setups used as well as imperfections in the SIM reconstruction and image stitching processes.
168 While these artifacts are sometimes minimal enough to remain uncorrected, certain artifacts seriously inhibit the
169 usefulness of the final stitched image. In [23], the authors note that issues in triggering and evenly illuminating the
170 microdisplay being used for illumination resulted in striping and vignetting artifacts; similarly, in [22,24,36,52],
171 stitching artifacts are apparent in the images. Here, optimization of the optical setup, camera-microdisplay
172 synchronization, and image processing methods yielded whole-slide images free from visible SIM or image stitching
173 artifacts. In addition to the elimination of artifacts, our use of SIMToolbox to perform SIM reconstruction on the
174 data allows for a variety of reconstruction algorithms to be used, including super-resolution algorithms such as
175 MAP-SIM. This too presents an improvement over previous works. Our methods also allow for stitching of high-
176 magnification tiles into large-FOV images with subdiffractive detail (see supplementary Fig. S3).

177 Another advantage of the acquisition and processing methods demonstrated here is the minimization of
178 user intervention, and in turn, reductions in acquisition and processing time. Firstly, the use of Andor IQ during
179 acquisition allows for stage movement, sample focusing, image acquisition, and SIM pattern advancement to be
180 controlled automatically. Loading of the sample, definition of the mosaic edges, and manual focus on 3-5 positions
181 of the sample are the only steps needed to be taken by the user before acquisition can begin. Recent developments in
182 autofocus technology for SIM may allow for the manual focus step to be shortened or omitted [52]. These automated
183 steps during acquisition allow for large mosaics to be acquired. The quality of the final stitched images does not
184 degrade for larger mosaics – in fact, the quality of the devignetting process improves with larger datasets, as more
185 data is available to produce an accurate estimation of the illumination profile. SIMToolbox (version 2.0), which is
186 capable of utilizing the processing power of modern consumer graphics cards during MAP-SIM processing, also
187 reduces the time spent during the data processing phase. Finally, unlike other super-resolution reconstruction

188 methods such as SR-SIM, MAP-SIM is able to produce artifact-free results without tuning of reconstruction
189 parameters by the user, a process which is difficult to automate and requires significant user experience.

190 One drawback the method presented here is the inability to image the entire volume of samples thicker than
191 ~0.5 mm. However, this limitation does not prevent large, unsectioned samples from being imaged, as is the case
192 with bright field microscopy, where samples must be thin enough for transmitted light to reach the objective. Rather,
193 as the light which illuminates the sample in fluorescence microscopy emanates from the objective, all surface
194 regions of a large sample may be imaged. Additionally, due to the optical sectioning exhibited by SIM, light from
195 out-of-focus regions of the sample is almost completely attenuated. Consequently, imaging the surfaces of large
196 samples with SIM produces high-contrast images of thin regions without the need for physical sectioning, as
197 previously demonstrated [23,36].

198 Here, we demonstrated our imaging techniques on traditionally prepared histopathological samples in order
199 to provide a comparison between bright field imaging and SIM, but the same techniques can be used to image a
200 wide variety of fluorescently labelled samples, as demonstrated in the supplementary material. The ability to
201 seamlessly image the entire surface region of large samples has multiple potential applications in histopathology.
202 SIM presents unique advantages in analyzing the surgical margins of large tissue excisions, as demonstrated by
203 Wang [36]. Briefly, due to the ability of SIM to image an unsectioned sample, analysis of surgical margins using
204 SIM requires imaging of far less surface area than that needed for bright field imaging. Confocal imaging of core
205 needle biopsy samples has been previously demonstrated to produce images suitable for medical diagnosis [42], a
206 practice easily adapted to SIM. The speed at which sample preparation and image acquisition can be performed in
207 fluorescence microscopy presents opportunities for intra-operative analysis of tissue samples using SIM techniques,
208 as mentioned by multiple other studies [23,36,53,54].

209 **Reuse potential**

210 The data provided here presents various opportunities for reuse. Firstly, the unstitched image tiles of the
211 basal cell carcinoma sample provided in the dataset, which still contain vignetting artifacts, may be used to
212 reproduce the results of our devignetting process, as well as to further develop more sophisticated devignetting
213 approaches suited for SIM. These tiles might also be used to create or modify existing stitching software for global
214 minimization of stitching artifacts. For example, the frequency-domain detection of periodic stitching artifacts

215 discussed in the supplementary material could be used to minimize such artifacts in developing new stitching
216 software. Note that the image tiles from the other samples in the dataset are provided after deconvolution. With the
217 multiple high-resolution color overviews and stitched SIM images, comparison of structures visible in the brightfield
218 and fluorescent images could be performed to further study the use of fluorescence microscopy in histopathology.

219 **Availability of source code and requirements**

220 Project name: SIMToolbox version 2.12

221 Project home page: <http://mmtg.fel.cvut.cz/SIMToolbox/>

222 Operating system: platform independent

223 Programming language: MATLAB

224 License: GNU General Public License v3.0

225 **Detailed software compatibility notes**

226 The SIMToolbox GUI was compiled with MATLAB 2015a and tested in Windows 7 and 8. The GUI is a stand-alone
227 program and does not require MATLAB to be installed. To use the MATLAB functions within SIMToolbox (i.e.,
228 without the GUI), MATLAB must be installed. The functions were mainly developed with 64 bit MATLAB versions
229 2012b, 2014a, 2015a in Windows 7. When using SIMToolbox functions without the GUI, the MATLAB “Image
230 Processing Toolbox” is required. SIMToolbox also requires the “MATLAB YAML” package to convert MATLAB
231 objects to/from YAML file format. Note that this package is installed automatically when using the GUI.

232 **Availability of data**

233 All raw and analyzed data is available on GigaDB at <http://gigadb.org/site/index>.

234 **Abbreviations**

235 Av Int Proj, average intensity projection; FOV, field of view; H&E, hematoxylin and eosin; ICE, Image Composite
236 Editor; MAP-SIM, maximum *a posteriori* probability SIM; NA, numerical aperture; LCOS, liquid crystal on silicon;
237 PSDca, circularly averaged power spectral density; SIM, structured illumination microscopy; WF, wide field.

238 **Ethics approval and consent to participate**

239 Not applicable

240 **Consent for publication**

241 Not applicable

242 **Competing interests**

243 The authors declare that they have no competing interests.

244 **Funding**

245 Research reported in this publication was supported by the National Institute of General Medical Sciences of the
246 National Institutes of Health under award number 1R15GM128166-01. This work was also supported by the UCCS
247 center for the University of Colorado BioFrontiers Institute. The funding sources had no involvement in study design;
248 in the collection, analysis and interpretation of data; in the writing of the report; or in the decision to submit the article
249 for publication. This material is based in part upon work supported by the National Science Foundation under Grant
250 Number 1727033. Any opinions, findings, and conclusions or recommendations expressed in this material are those
251 of the authors and do not necessarily reflect the views of the National Science Foundation.

252 **Author Contributions**

253 KJ: acquired data, analyzed data, wrote the paper

254 GH: conceived project, acquired data, analyzed data, supervised research, wrote the paper

255 **References**

- 256 1. M. A. A. Neil, R. Juškaitis, and T. Wilson, "Method of obtaining optical sectioning by using structured light
257 in a conventional microscope," *Opt. Lett.* **22**, 1905–1907 (1997).
- 258 2. M. G. L. Gustafsson, "Surpassing the lateral resolution limit by a factor of two using structured illumination
259 microscopy," *J. Microsc.* **198**, 82–87 (2000).
- 260 3. R. Heintzmann and C. Cremer, "Laterally modulated excitation microscopy: improvement of resolution by
261 using a diffraction grating," *Proc. SPIE* **3568**, 185–196 (1998).
- 262 4. L. Schermelleh, P. M. Carlton, S. Haase, L. Shao, L. Winoto, P. Kner, B. Burke, M. C. Cardoso, D. A.
263 Agard, M. G. L. Gustafsson, H. Leonhardt, and J. W. Sedat, "Subdiffraction multicolor imaging of the
264 nuclear periphery with 3D structured illumination microscopy," *Science (80-.)*. **320**, 1332–1336 (2008).
- 265 5. R. Fiolka, L. Shao, E. H. Rego, M. W. Davidson, and M. G. L. Gustafsson, "Time-lapse two-color 3D
266 imaging of live cells with doubled resolution using structured illumination," *Proc. Natl. Acad. Sci. U. S. A.*
267 **109**, 5311–5315 (2012).
- 268 6. J. Pospíšil, T. Lukeš, J. Bendesky, K. Fliegel, K. Spendier, and G. M. Hagen, "Imaging tissues and cells
269 beyond the diffraction limit with structured illumination microscopy and Bayesian image reconstruction,"
270 *Gigascience* **8**, giy126 (2019).

- 271 7. X. Huang, J. Fan, L. Li, H. Liu, R. Wu, Y. Wu, L. Wei, H. Mao, A. Lal, P. Xi, L. Tang, Y. Zhang, Y. Liu, S.
272 Tan, and L. Chen, "Fast, long-term, super-resolution imaging with Hessian structured illumination
273 microscopy," *Nat. Biotechnol.* (2018).
- 274 8. M. G. L. Gustafsson, L. Shao, P. M. Carlton, C. J. R. Wang, I. N. Golubovskaya, W. Z. Cande, D. A. Agard,
275 and J. W. Sedat, "Three-dimensional resolution doubling in widefield fluorescence microscopy by structured
276 illumination," *Biophys. J.* **94**, 4957–4970 (2008).
- 277 9. S. Rossberger, G. Best, D. Baddeley, R. Heintzmann, U. Birk, S. Dithmar, and C. Cremer, "Combination of
278 structured illumination and single molecule localization microscopy in one setup," *J. Opt.* **15**, 094003
279 (2013).
- 280 10. P. Křížek, I. Raška, and G. M. Hagen, "Flexible structured illumination microscope with a programmable
281 illumination array," *Opt. Express* **20**, 24585 (2012).
- 282 11. P. Kner, B. B. Chhun, E. R. Griffis, L. Winoto, and M. G. L. Gustafsson, "Super-resolution video
283 microscopy of live cells by structured illumination," *Nat. Methods* **6**, 339–342 (2009).
- 284 12. L. J. Young, F. Ströhl, and C. F. Kaminski, "A Guide to Structured Illumination TIRF Microscopy at High
285 Speed with Multiple Colors," *J. Vis. Exp.* e53988–e53988 (2016).
- 286 13. V. Poher, H. X. Zhang, G. T. Kennedy, C. Griffin, S. Oddos, E. Gu, D. S. Elson, M. Girkin, P. M. W.
287 French, M. D. Dawson, and M. A. Neil, "Optical sectioning microscope with no moving parts using a micro-
288 stripe array light emitting diode," *Opt. Express* **15**, 11196–11206 (2007).
- 289 14. F. Orieux, E. Sepulveda, V. Loriette, B. Dubertret, and J.-C. Olivo-Marin, "Bayesian estimation for
290 optimized structured illumination microscopy," *IEEE Trans. Image Process.* **21**, 601–14 (2012).
- 291 15. T. Lukeš, P. Křížek, Z. Švindrych, J. Benda, M. Ovesný, K. Fliegel, M. Klíma, and G. M. Hagen, "Three-
292 dimensional super-resolution structured illumination microscopy with maximum a posteriori probability
293 image estimation," *Opt. Express* **22**, 29805–17 (2014).
- 294 16. T. Lukeš, G. M. Hagen, P. Křížek, Z. Švindrych, M. Klíma, and K. Fliegel, "Comparison of image
295 reconstruction methods for structured illumination microscopy," *Proc. SPIE* **9129**, 91293J (2014).
- 296 17. C. A. Werley, M.-P. Chien, and A. E. Cohen, "An ultrawidefield microscope for high-speed fluorescence
297 imaging and targeted optogenetic stimulation," *Biomed. Opt. Express* **8**, 5794 (2017).
- 298 18. N. J. Sofroniew, D. Flickinger, J. King, and K. Svoboda, "A large field of view two-photon mesoscope with

- 299 subcellular resolution for in vivo imaging," *Elife* **5**, (2016).
- 300 19. G. McConnell, J. Trägårdh, R. Amor, J. Dempster, E. Reid, and W. B. Amos, "A novel optical microscope
301 for imaging large embryos and tissue volumes with sub-cellular resolution throughout," *Elife* **5**, (2016).
- 302 20. P. J. Keller, A. D. Schmidt, J. Wittbrodt, and E. H. K. Stelzer, "Reconstruction of zebrafish early embryonic
303 development by scanned light sheet microscopy," *Science* (80-.). **322**, 1065–1069 (2008).
- 304 21. J. N. Stirman, I. T. Smith, M. W. Kudenov, and S. L. Smith, "Wide field-of-view, multi-region, two-photon
305 imaging of neuronal activity in the mammalian brain," *Nat. Biotechnol.* **34**, 857–862 (2016).
- 306 22. B. Migliori, M. S. Datta, C. Dupre, M. C. Apak, S. Asano, R. Gao, E. S. Boyden, O. Hermanson, R. Yuste,
307 and R. Tomer, "Light sheet theta microscopy for rapid high-resolution imaging of large biological samples,"
308 *BMC Biol.* **16**, 57 (2018).
- 309 23. T. C. Schlichenmeyer, M. Wang, K. N. Elfer, and J. Q. Brown, "Video-rate structured illumination
310 microscopy for high-throughput imaging of large tissue areas," *Biomed. Opt. Express* **5**, 366 (2014).
- 311 24. D. Xu, T. Jiang, A. Li, B. Hu, Z. Feng, H. Gong, S. Zeng, and Q. Luo, "Fast optical sectioning obtained by
312 structured illumination microscopy using a digital mirror device," *J. Biomed. Opt.* **18**, 060503 (2013).
- 313 25. F. B. Legesse, O. Chernavskaja, S. Heuke, T. Bocklitz, T. Meyer, J. Popp, and R. Heintzmann, "Seamless
314 stitching of tile scan microscope images," *J. Microsc.* **258**, 223–232 (2015).
- 315 26. S. Preibisch, S. Saalfeld, and P. Tomancak, "Globally optimal stitching of tiled 3D microscopic image
316 acquisitions," *Bioinformatics* **25**, 1463–1465 (2009).
- 317 27. C. Murtin, C. Frindel, D. Rousseau, and K. Ito, "Image processing for precise three-dimensional registration
318 and stitching of thick high-resolution laser-scanning microscopy image stacks," *Comput. Biol. Med.* **92**, 22–
319 41 (2018).
- 320 28. J. Chalfoun, M. Majurski, T. Blattner, K. Bhadriraju, W. Keyrouz, P. Bajcsy, and M. Brady, "MIST:
321 Accurate and Scalable Microscopy Image Stitching Tool with Stage Modeling and Error Minimization," *Sci.*
322 *Rep.* **7**, 4988 (2017).
- 323 29. Y. Yu and H. Peng, "Automated high speed stitching of large 3D microscopic images," in *2011 IEEE*
324 *International Symposium on Biomedical Imaging: From Nano to Macro* (IEEE, 2011), pp. 238–241.
- 325 30. A. Bria and G. Iannello, "TeraStitcher - A tool for fast automatic 3D-stitching of teravoxel-sized microscopy
326 images," *BMC Bioinformatics* **13**, 316 (2012).

- 327 31. F. Yang, Z.-S. Deng, and Q.-H. Fan, "A method for fast automated microscope image stitching," *Micron* **48**,
328 17–25 (2013).
- 329 32. P. Thévenaz and M. Unser, "User-friendly semiautomated assembly of accurate image mosaics in
330 microscopy," *Microsc. Res. Tech.* **70**, 135–146 (2007).
- 331 33. P. Křížek, T. Lukeš, M. Ovesný, K. Fliegel, and G. M. Hagen, "SIMToolbox: A MATLAB toolbox for
332 structured illumination fluorescence microscopy," *Bioinformatics* **32**, 318–320 (2015).
- 333 34. Microsoft, "Image Composite Editor," [https://www.microsoft.com/en-us/research/product/computational-
334 photography-applications/image-composite-editor/#!/support](https://www.microsoft.com/en-us/research/product/computational-photography-applications/image-composite-editor/#!/support).
- 335 35. C. A. Schneider, W. S. Rasband, and K. W. Eliceiri, "NIH Image to ImageJ: 25 years of image analysis.,"
336 *Nat. Methods* **9**, 671–5 (2012).
- 337 36. M. Wang, D. B. Tulman, A. B. Sholl, H. Z. Kimbrell, S. H. Mandava, K. N. Elfer, S. Luethy, M. M.
338 Maddox, W. Lai, B. R. Lee, and J. Q. Brown, "Gigapixel surface imaging of radical prostatectomy
339 specimens for comprehensive detection of cancer-positive surgical margins using structured illumination
340 microscopy," *Sci. Rep.* **6**, 27419 (2016).
- 341 37. J. L. Dobbs, H. Ding, A. P. Benveniste, H. M. Kuerer, S. Krishnamurthy, W. Yang, and R. Richards-
342 Kortum, "Feasibility of confocal fluorescence microscopy for real-time evaluation of neoplasia in fresh
343 human breast tissue," *J. Biomed. Opt.* **18**, 106016 (2013).
- 344 38. D. S. Gareau, "Feasibility of digitally stained multimodal confocal mosaics to simulate histopathology," *J.*
345 *Biomed. Opt.* **14**, 034050 (2009).
- 346 39. M. T. Tilli, M. C. Cabrera, A. R. Parrish, K. M. Torre, M. K. Sidawy, A. L. Gallagher, E. Makariou, S. A.
347 Polin, M. C. Liu, and P. A. Furth, "Real-time imaging and characterization of human breast tissue by
348 reflectance confocal microscopy," *J. Biomed. Opt.* **12**, 051901 (2007).
- 349 40. A. Parrish, E. Halama, M. T. Tilli, M. Freedman, and P. A. Furth, "Reflectance confocal microscopy for
350 characterization of mammary ductal structures and development of neoplasia in genetically engineered
351 mouse models of breast cancer," *J. Biomed. Opt.* **10**, 051602 (2005).
- 352 41. Y. Chen, W. Xie, A. K. Glaser, N. P. Reder, C. Mao, S. M. Dintzis, J. C. Vaughan, and J. T. C. Liu, "Rapid
353 pathology of lumpectomy margins with open-top light-sheet (OTLS) microscopy," *Biomed. Opt. Express*
354 **10**, 1257 (2019).

- 355 42. J. Dobbs, S. Krishnamurthy, M. Kyrish, A. P. Benveniste, W. Yang, and R. Richards-Kortum, "Confocal
356 fluorescence microscopy for rapid evaluation of invasive tumor cellularity of inflammatory breast carcinoma
357 core needle biopsies," *Breast Cancer Res. Treat.* **149**, 303–310 (2015).
- 358 43. G. M. Hagen, W. Caarls, K. A. Lidke, A. H. B. De Vries, C. Fritsch, B. G. Barisas, D. J. Arndt-Jovin, and T.
359 M. Jovin, "Fluorescence recovery after photobleaching and photoconversion in multiple arbitrary regions of
360 interest using a programmable array microscope," *Microsc. Res. Tech.* **72**, 431–440 (2009).
- 361 44. S. R. Kantelhardt, W. Caarls, A. H. B. de Vries, G. M. Hagen, T. M. Jovin, W. Schulz-Schaeffer, V. Rohde,
362 A. Giese, and D. J. Arndt-Jovin, "Specific Visualization of Glioma Cells in Living Low-Grade Tumor
363 Tissue," *PLoS One* **5**, e11323 (2010).
- 364 45. L. Shao, P. Kner, E. H. Rego, and M. G. L. Gustafsson, "Super-resolution 3D microscopy of live whole cells
365 using structured illumination," *Nat. Methods* **8**, 1044–1046 (2011).
- 366 46. B.-C. Chen, W. R. Legant, K. Wang, L. Shao, D. E. Milkie, M. W. Davidson, C. Janetopoulos, X. S. Wu, J.
367 A. Hammer, Z. Liu, B. P. English, Y. Mimori-Kiyosue, D. P. Romero, A. T. Ritter, J. Lippincott-Schwartz,
368 L. Fritz-Laylin, R. D. Mullins, D. M. Mitchell, J. N. Bembenek, A.-C. Reymann, R. Bohme, S. W. Grill, J.
369 T. Wang, G. Seydoux, U. S. Tulu, D. P. Kiehart, and E. Betzig, "Lattice light-sheet microscopy: Imaging
370 molecules to embryos at high spatiotemporal resolution," *Science* (80-.). **346**, 1257998 (2014).
- 371 47. G. M. Hagen, W. Caarls, M. Thomas, A. Hill, K. A. Lidke, B. Rieger, C. Fritsch, B. van Geest, T. M. Jovin,
372 and D. J. Arndt-Jovin, "Biological applications of an LCoS-based programmable array microscope (PAM),"
373 in D. L. Farkas, R. C. Leif, and D. V. Nicolau, eds. (2007), p. 64410S.
- 374 48. H. Hurwitz, "Entropy reduction in Bayesian analysis of measurements," *Phys. Rev. A* **12**, 698–706 (1975).
- 375 49. P. J. Verveer and T. M. Jovin, "Efficient superresolution restoration algorithms using maximum a posteriori
376 estimations with application to fluorescence microscopy," *J. Opt. Soc. Am. A* **14**, 1696 (1997).
- 377 50. Michael Schmid, "Fast Filters," https://imagejdocu.tudor.lu/plugin/filter/fast_filters/start.
- 378 51. K. Fliegel, M. Klíma, and J. Pospíšil, "Assessing resolution in live cell structured illumination microscopy,"
379 in *Photonics, Devices, and Systems VII*, P. Páta and K. Fliegel, eds. (SPIE, 2017), Vol. 10603, p. 39.
- 380 52. T. C. Schlichenmeyer, M. Wang, C. Wenk, J. Q. Brown, and J. Q. Brown, "Autofocus optimization for
381 tracking tissue surface topography in large-area mosaicking structured illumination microscopy," in
382 *Frontiers in Optics 2014* (OSA, 2014), p. FM4F.3.

- 383 53. H. L. Fu, J. L. Mueller, M. P. Javid, J. K. Mito, D. G. Kirsch, N. Ramanujam, and J. Q. Brown,
384 "Optimization of a Widefield Structured Illumination Microscope for Non-Destructive Assessment and
385 Quantification of Nuclear Features in Tumor Margins of a Primary Mouse Model of Sarcoma," *PLoS One* **8**,
386 e68868 (2013).
- 387 54. H. L. Fu, J. L. Mueller, M. J. Whitley, D. M. Cardona, R. M. Willett, D. G. Kirsch, J. Q. Brown, and N.
388 Ramanujam, "Structured Illumination Microscopy and a Quantitative Image Analysis for the Detection of
389 Positive Margins in a Pre-Clinical Genetically Engineered Mouse Model of Sarcoma," *PLoS One* **11**,
390 e0147006 (2016).

391 **FIGURE CAPTIONS**

392 Figure 1: Simplified diagram of SIM system. LCOS, liquid crystal on silicon

393 Figure 2: Vignetting artifacts and their removal. (a) shows the result of stitching images without applying the
394 devignetting process, while (b) shows a stitch of the same data after devignetting has been applied. (c) shows the
395 average intensity projection of the images used to stitch (a), which estimates the vignette profile of each frame. This
396 estimate can be refined by application of an edge-limited blurring filter, as shown in (d). (e) shows the average
397 intensity projection of the data used in (b), after devignetting has been applied. The uniform brightness of (e)
398 indicates that no major vignetting artifacts remain in the devignetted data.

399 Figure 3. Panoramic SIM data processing workflow. Devignetting was performed after SIM reconstruction. Note the
400 vignette profile differs between reconstruction methods, necessitating separate projection, blurring and division
401 steps. Av Int Proj refers to average intensity projection.

402 Figure 4. Evaluating image resolution. (a) and (b) show a tile from the data in Fig. 7 (basal cell carcinoma sample)
403 after widefield and MAP-SIM reconstruction, respectively. (c) and (d) each show a zoom-in of (a) and (b),
404 respectively. (e) and (f) each show the FFT of (a) and (b), respectively. The dotted lines in (e) and (f) indicate the
405 resolution of each image according to the resolution measurement described.

406 Figure 5. Normalized, radially averaged power spectral density (PSD_{ca}) and resolution analysis measured on the tiles
407 shown in Figs. 4a and 4b.

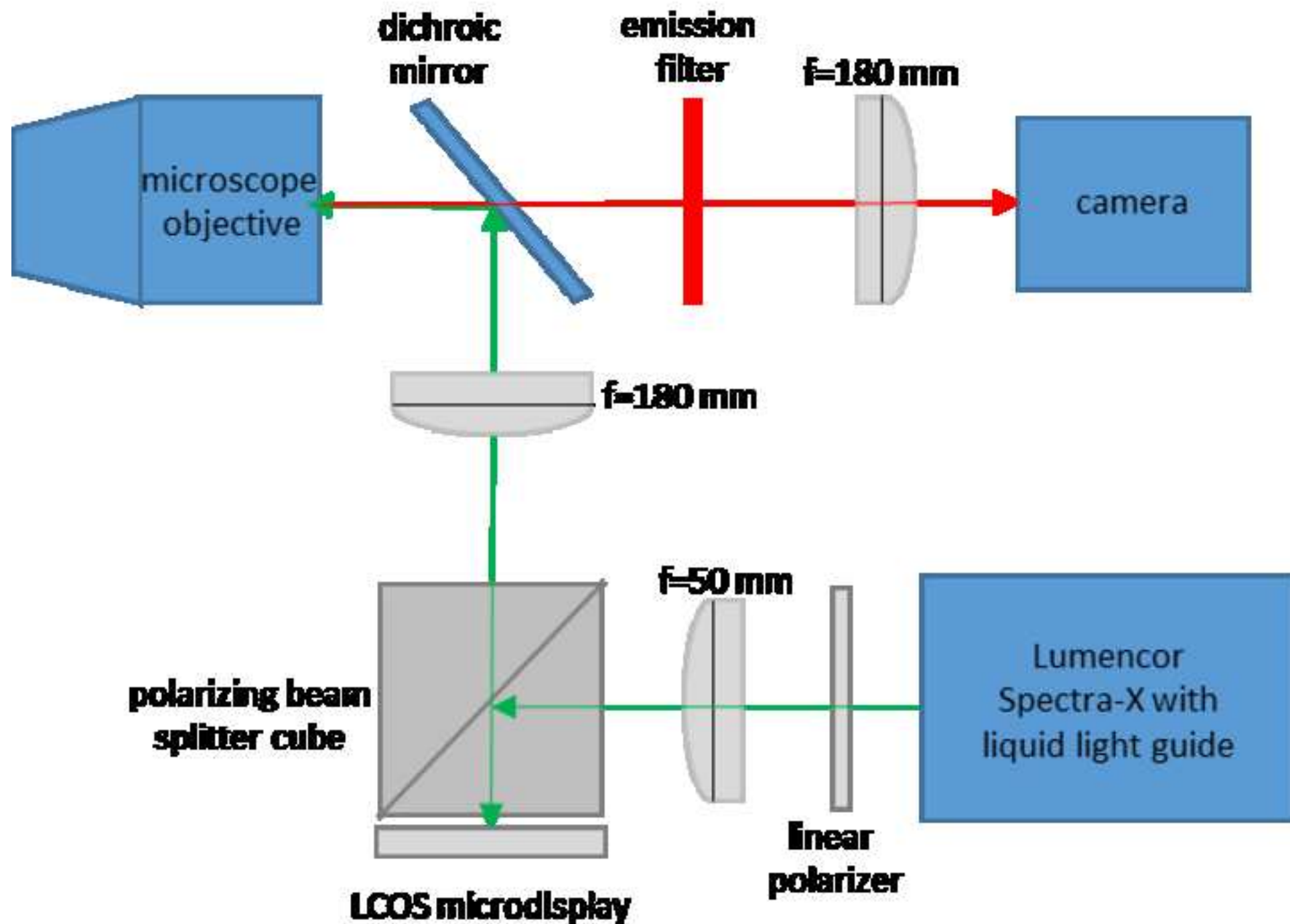
408 Figure 6: Carcinoma of human prostate. (a) Color overview, (b) WF stitch, (c) MAP-SIM stich. (d) shows a region
409 of the sample indicated in (a). (e) and (f) each show a zoom-in of (b) and (c), respectively, in the region indicated in
410 (a).

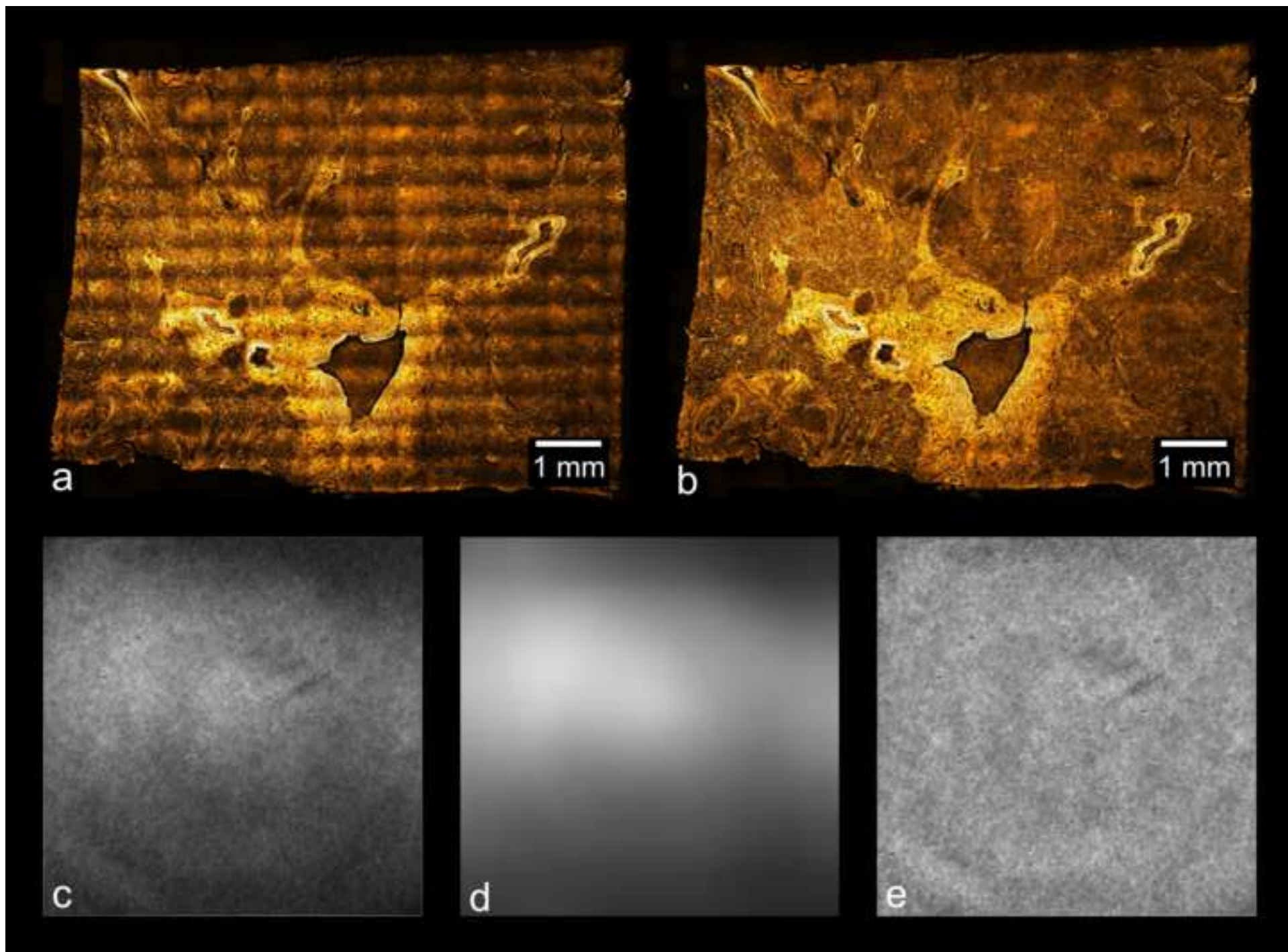
411 Figure 7: Basal Cell Carcinoma. (a) Color overview, (b) WF stitch, (c) MAP-SIM stich. (d) shows a region of the
412 sample indicated in (a). (e) and (f) each show a zoom-in of (b) and (c), respectively, in the region indicated in (a).

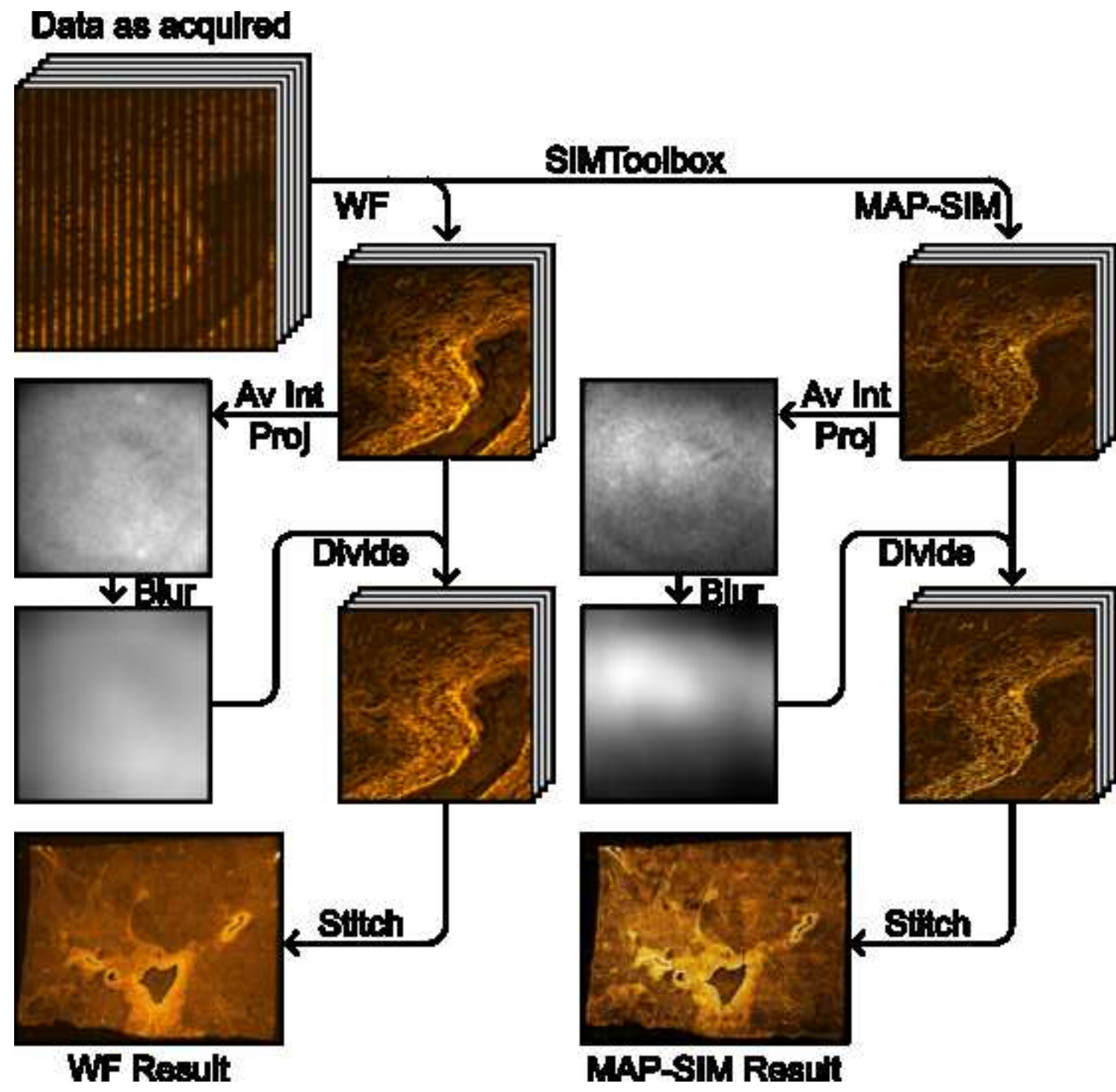
413 Figure 8: Adenocarcinoma of human ovary. (a) Color overview, (b) WF stitch, (c) MAP-SIM stich. (d), (g) show a
414 region of the sample indicated in (a), acquired separately from (a) using a 10× objective. (e) and (h) show a zoom-in
415 of (b), while (f) and (i) show a zoom-in of (c), all in the regions indicated in (a).

416 Figure 9: Adenocarcinoma of human breast. (a) Color overview, (b) WF stitch, (c) MAP-SIM stich. (d) shows a
417 region of the sample indicated in (a), acquired separately from (a) using a 10× objective. (e) and (f) each show a
418 zoom-in of (b) and (c), respectively, in the region indicated in (a).

419 Figure 10: Tuberculosis of human lung. (a) Color overview, (b) WF stitch, (c) MAP-SIM stich. (d) shows a region
420 of the sample indicated in (a), acquired separately from (a) using a 20× objective. (e) and (f) each show a zoom-in of
421 (b) and (c), respectively, in the region indicated in (a).







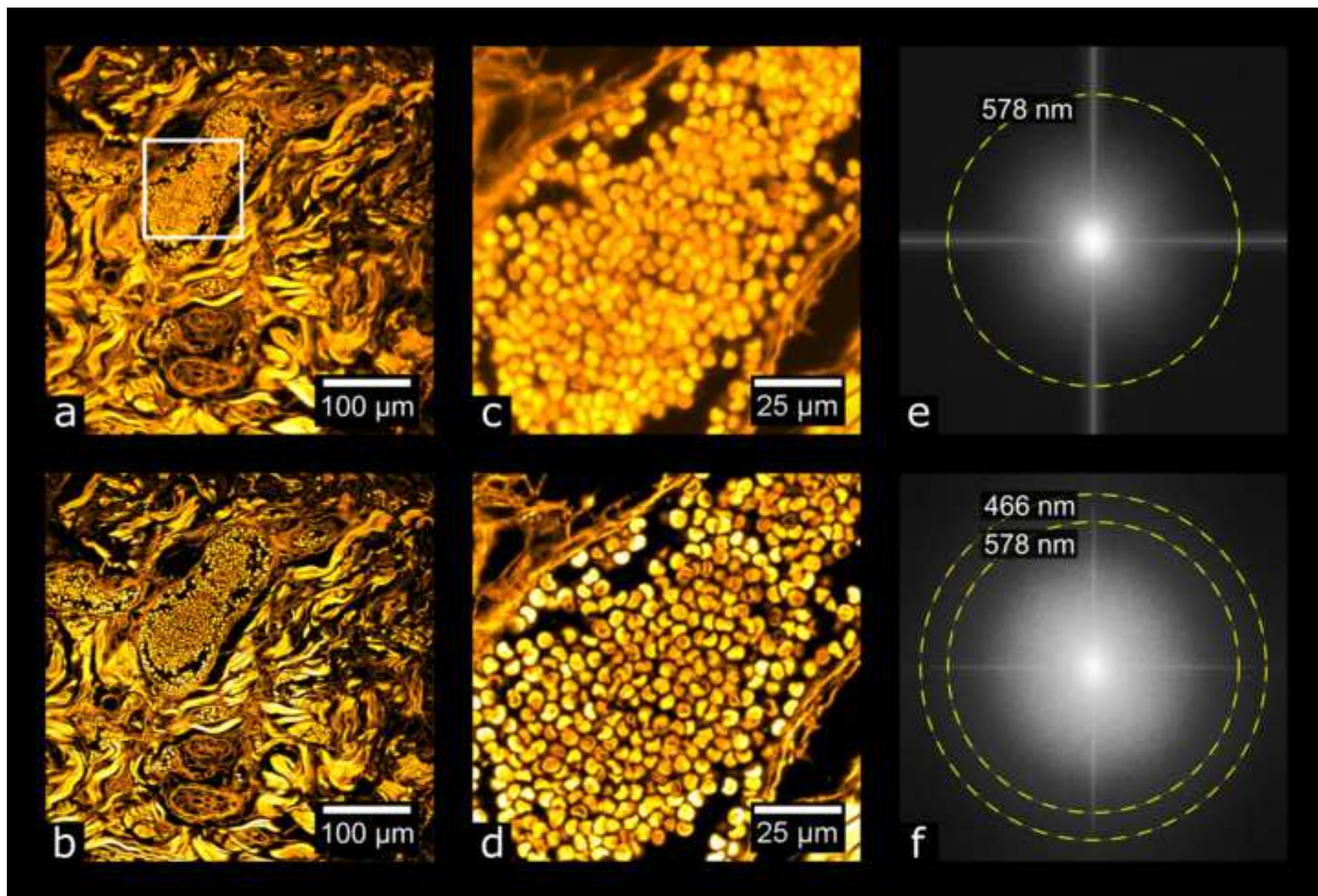
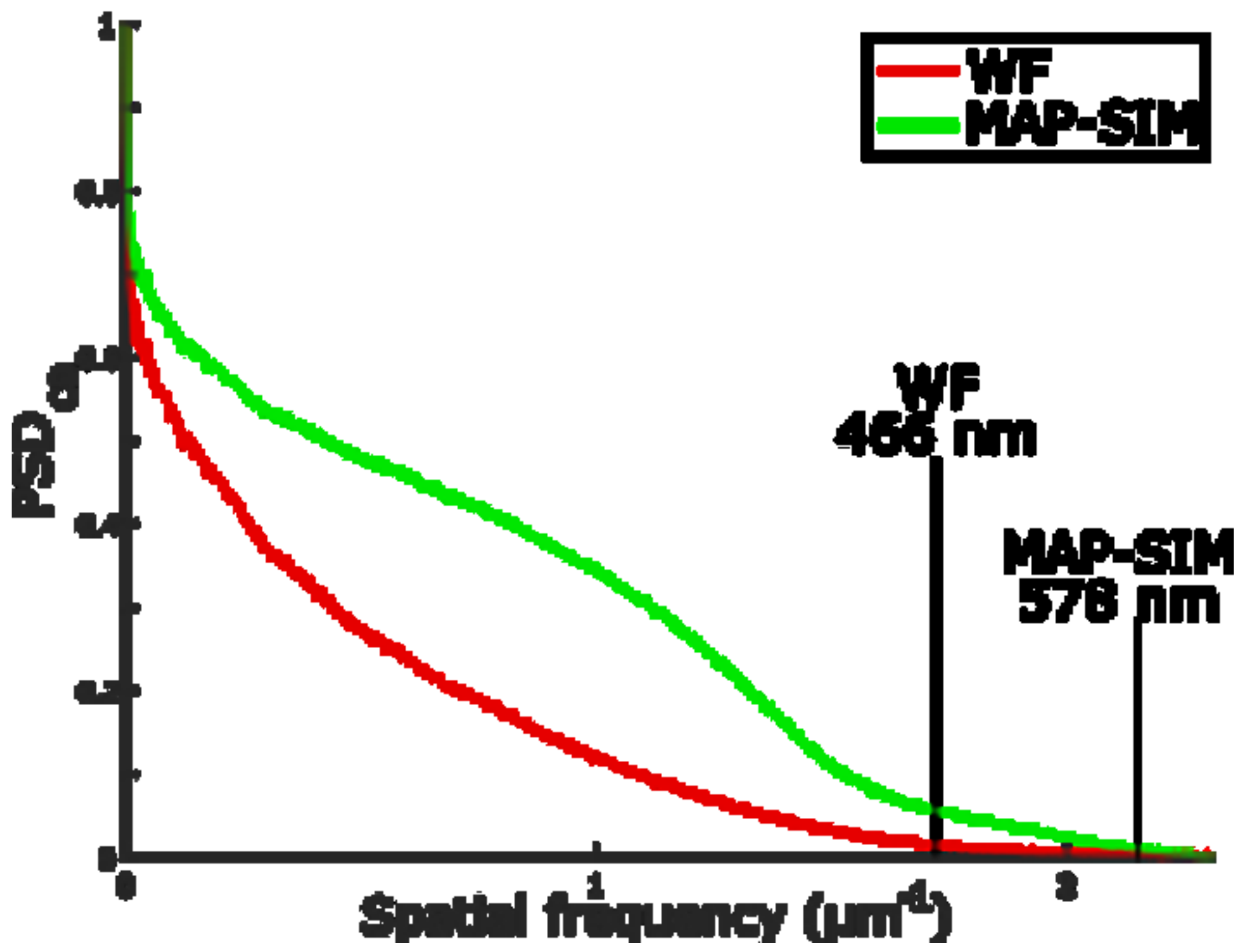
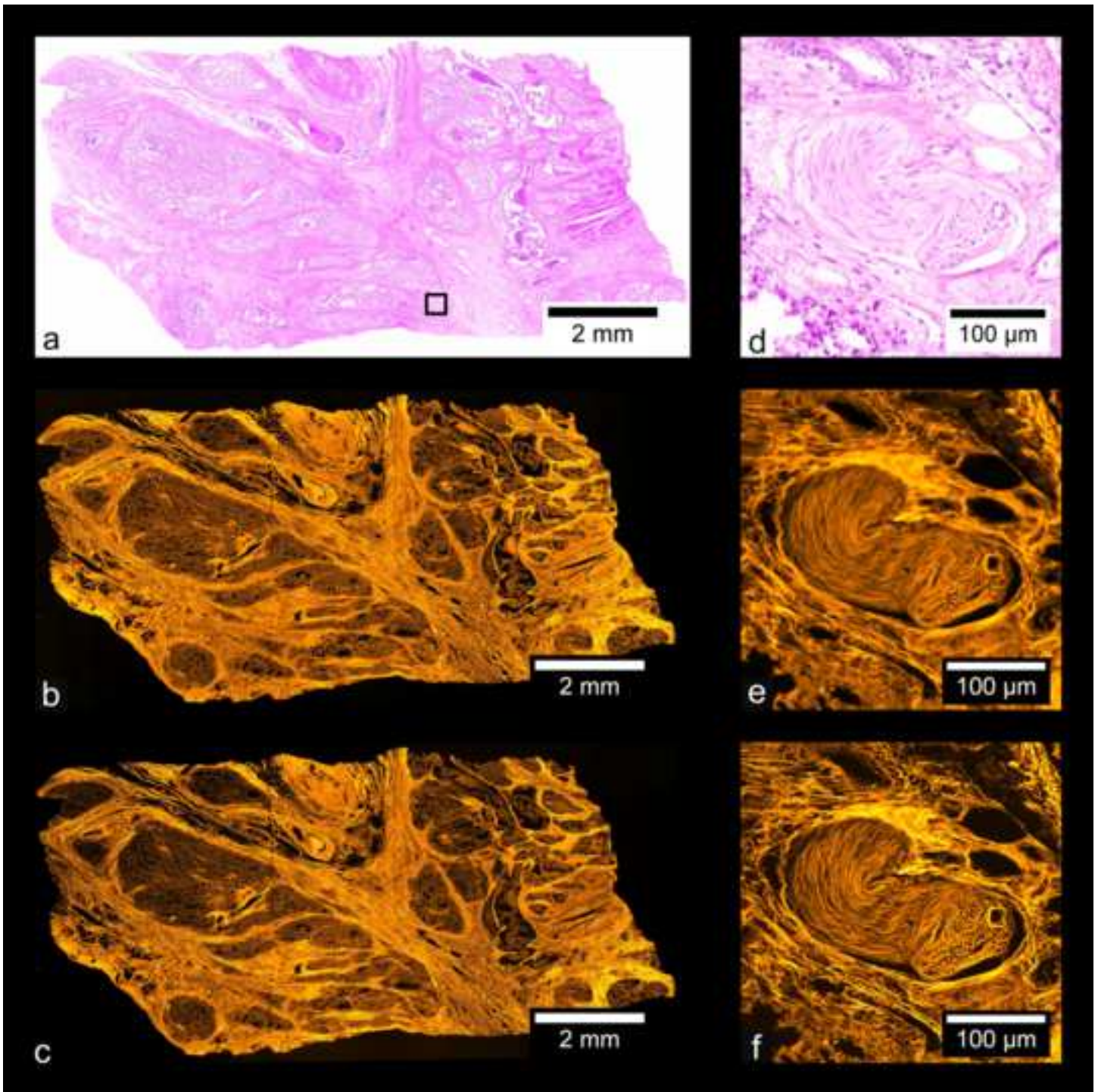
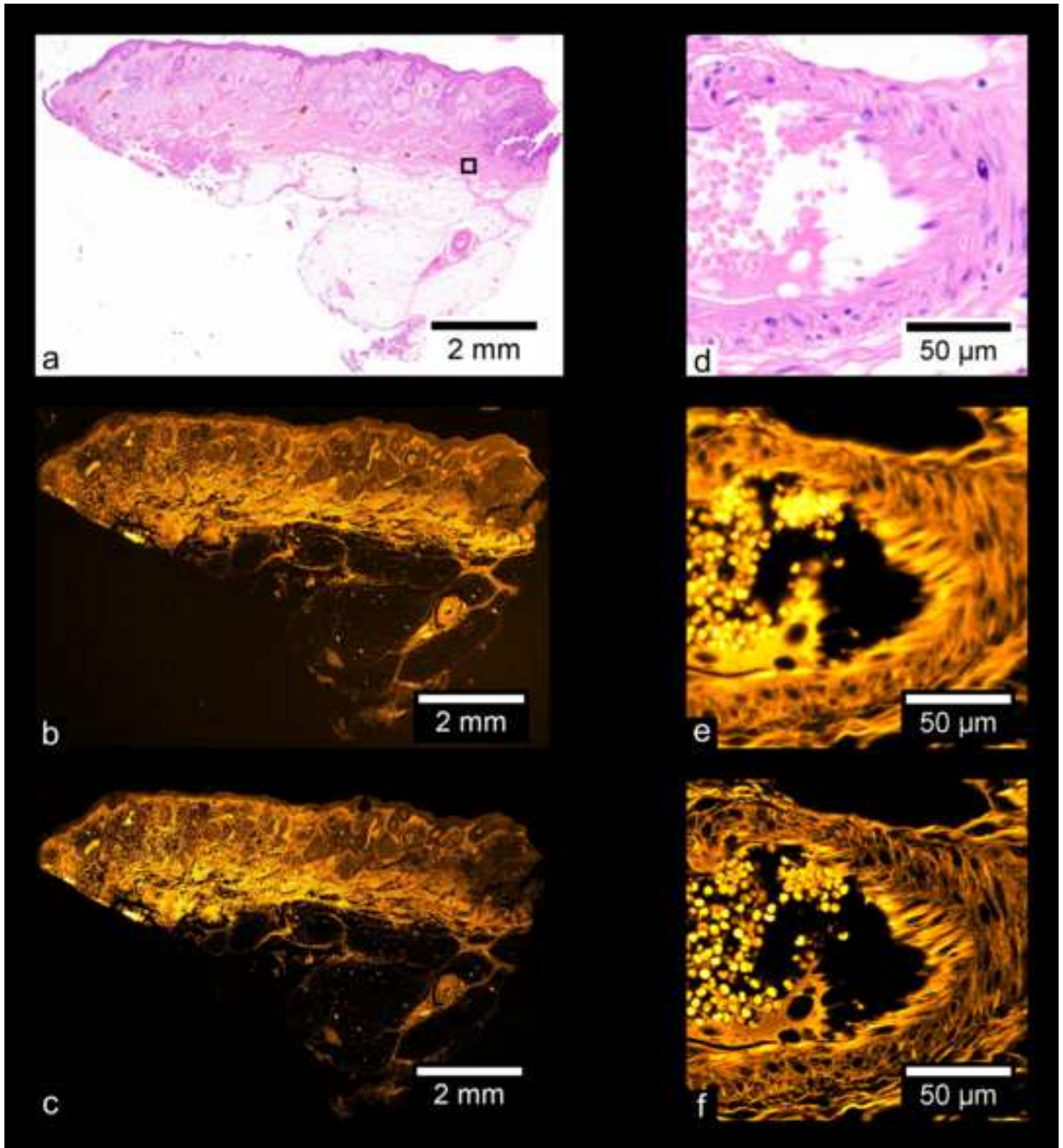
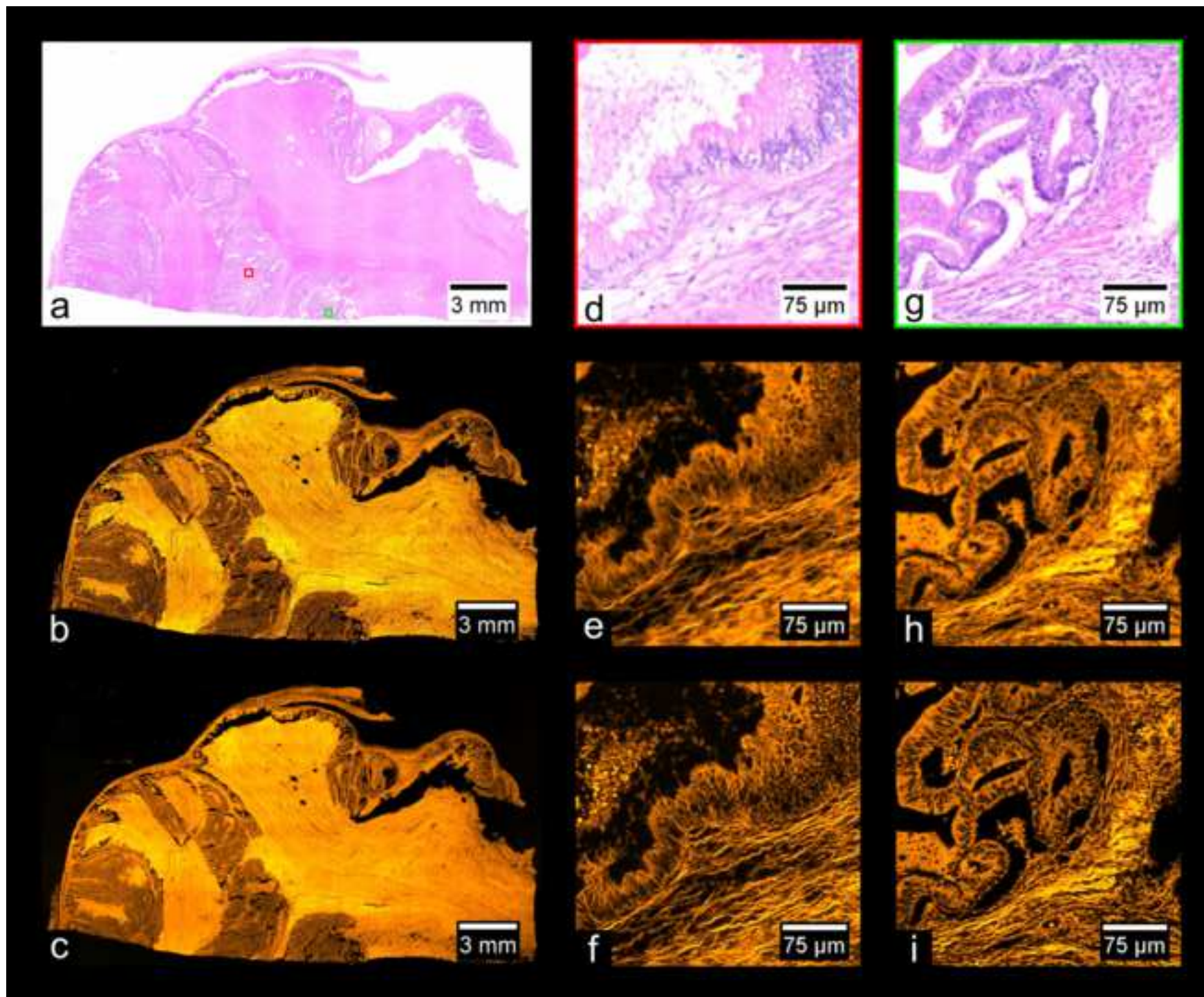


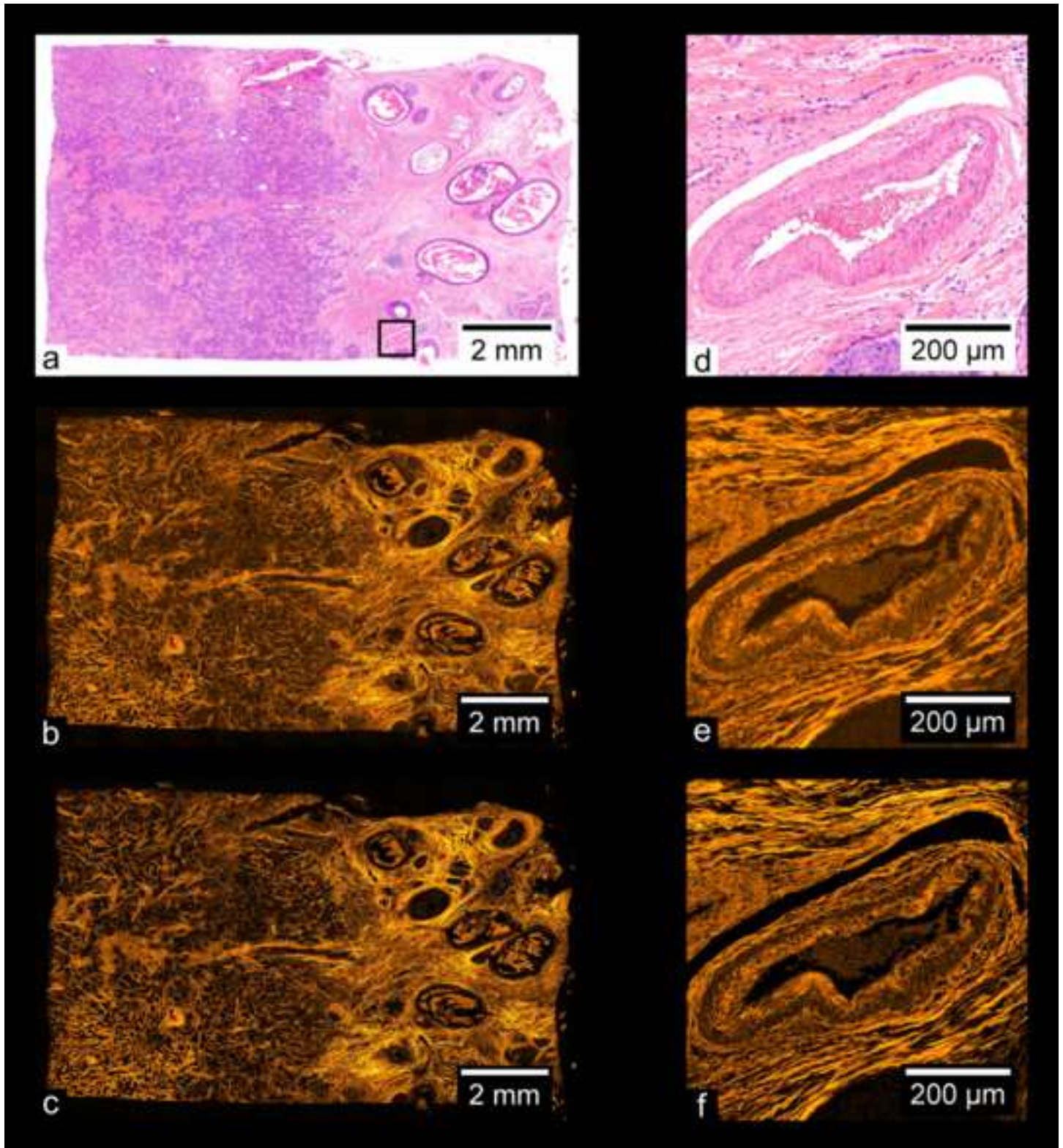
Figure 5

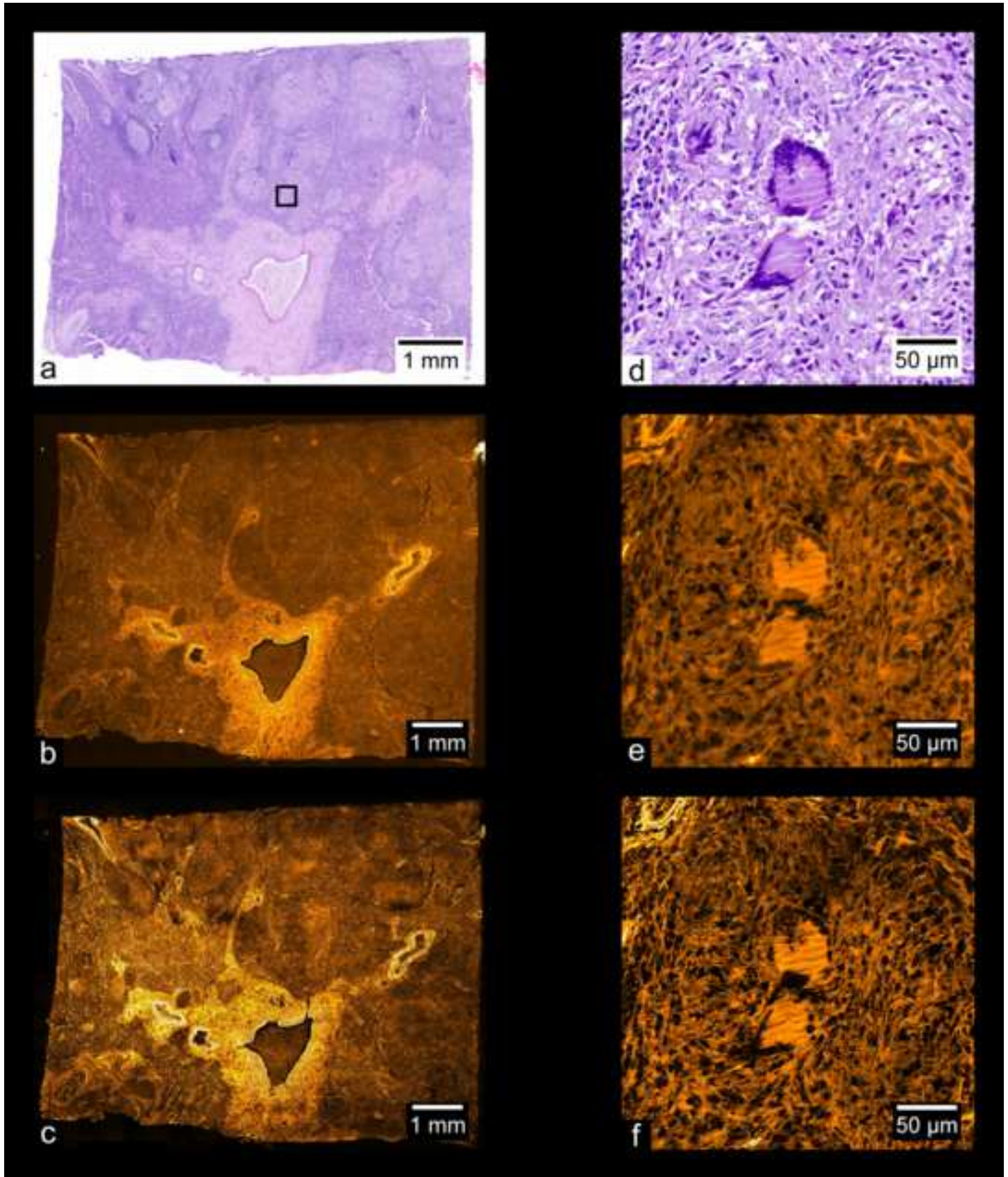














Click here to access/download
Supplementary Material
Supplement.docx





University of Colorado
Colorado Springs

Dr. Guy M. Hagen

Biofrontiers

1420 Austin Bluffs Pkwy.

Colorado Springs, CO 80918

Tel. 719-255-3692

ghagen@uccs.edu

Dear Editor:

We would like to re-submit our manuscript entitled “Artifact-free whole-slide imaging with structured illumination microscopy and Bayesian image reconstruction” for consideration in *GigaScience* as a data note. We would like to thank the reviewers for their comments about the paper. Reviewer 1 was very enthusiastic about the paper and we appreciate these positive comments about our work. Reviewer 2 was also positive, but had a few comments about the paper which were concerned with the organization of the paper and the data.

1. The first comment was that we should upload all of the un-stitched images, and to provide them as individual image files rather than as a single large file. This has been accomplished and now all of the raw and processed data is available at GigaDB. We packed all of the tiles for a given sample into ZIP files so that users will be able to download all of the tiles as a single large file. Otherwise users would have to click and download each file separately. GigaDB will probably re-package these files into a different format such as TAR.

2. The reviewer noted that we did not include certain information about the actual dataset in the main paper. For example, the directory structure, file sizes and types, etc. This information is not normally included in GigaScience articles which I have read. The GigaScience Instructions to Authors do not require this information. This information will be present on the GigaDB page for this dataset. There will be a table, generated by GigaDB, which will contain the desired information.

3. The reviewer noted that an open access dedication should be included with the dataset. This has been done.

4. The reviewer noted that, because the tissue preparations are of human origin, that information about ethics and consent should not be overlooked. Thank you for reminding us of this important point. However, because the samples were obtained commercially, it is the responsibility of the supplying company to ensure that ethical and legal guidelines are followed. I have double checked this with the Institutional Review Board (IRB) here at the University of Colorado, Colorado Springs. Because the samples are acquired commercially, and because they are completely de-identified (meaning that there is no way to connect these particular samples to the original donor), this is not considered human subject research, and approval is not required to work with these samples.

5, 6. In points 5 and 6, the reviewer is asking us to rearrange the paper by putting the items in the supplementary information into the main paper, and then to eliminate figures 7-10. Respectfully, we do not plan to do this for several reasons. I feel that reorganizing the manuscript as suggested would not improve the paper.

The whole point of the paper is to show the results of our research, in this case the results are the final, high resolution stitched images of the samples we examined. Eliminating these results from the paper would not be a good idea. For example, people working on breast cancer will be interested in the imaged breast cancer sample, people working on prostate cancer will be interested in the imaged prostate



University of Colorado
Colorado Springs

Dr. Guy M. Hagen

Biofrontiers

1420 Austin Bluffs Pkwy.

Colorado Springs, CO 80918

Tel. 719-255-3692

ghagen@uccs.edu

cancer sample, and so on. Further, the data re-use section was included in the supplementary material in our previous two papers in GigaScience. I believe this is the appropriate place for this information. Most GigaScience articles I have read do not include an actual, concrete example of data re-use like we do, and so this is a strength of our paper. Not everything can go into the main paper, and it is common practice today to publish supplementary information with additional experimental details, which can sometimes be quite lengthy.

Section 3 of the supplementary information is there for a specific reason. Almost all current research in structured illumination microscopy is performed on single cells using high magnification objectives. In the current paper we are imaging tissues over large areas, which is a quite different application. It is important for readers to realize that the methods presented here are widely applicable, including in the more typical application of SIM. Section 3 of the supplement is aimed at other people involved in the SIM field.

7. The structured illumination data processing steps are the same as were used in our previous publications. We noted this in the section 'SIM data processing' by stating that the SIM reconstructions were performed in the same way as previously described. What is new here is the image deconvolution and stitching methods applied to microscopy images of this type.

The steps described in the flow chart in Fig 3 are already described in the text. For example in the section 'SIM data processing' we state "SIM reconstructions were performed using SIMToolbox..." and "We generated optically sectioned, enhanced resolution images using... MAP-SIM." In the section 'Vignetting correction' we state "Following SIM reconstruction, ...We performed vignette removal by dividing each tile of the mosaic by an image representing the vignetting profile common to all tiles." These are exactly the steps shown in the flowchart.

8. The reviewer noted that the quality of figures 1, 3, and 5 is very low. This is perfectly true, in the PDF file they look absolutely terrible and it is very disappointing. However the problem is with the PDF conversion process used by GigaScience. This is not something that authors can change. Please click on the links embedded in the PDF (in the upper right corner of the pages containing the figures) to download the original high resolution files for the figures. You will see that they are of high quality.

We hope that our paper will now be acceptable for publication in GigaScience.

Sincerely,

A handwritten signature in blue ink that reads "Guy Hagen". The signature is fluid and cursive, with a long horizontal stroke at the end.

Guy M. Hagen